PHILOSOPHICAL TRANSACTIONS OF THE ROYAL SOCIETY A MATHEMATICAL, PHYSICAL & ENGINEERING SCIENCES

Turbulent closure and the modelling of fire by using computational fluid dynamics

G. Cox

Phil. Trans. R. Soc. Lond. A 1998 **356**, 2835-2854
doi: 10.1098/rsta.1998.0300

THE ROYAL SOCIETY

Turbulent closure and the modelling of fire by using computational fluid dynamics

By G. Cox

Fire Research Station, Building Research Establishment, Garston WD2 7JR, UK

The consequences of fluctuation and intermittency in the velocity and scalar properties of fires are examined from the perspective of their modelling by using computational fluid dynamics. The effects of interactions of turbulence with reaction kinetics, soot formation and radiant heat transfer are discussed, and illustrations are provided of the application of various closures, simple and complex, to the problems of smoke movement and solid-phase combustion.

Keywords: fire; smoke; fire modelling; computational fluid dynamics (CFD)

1. Introduction

In the late 1960s and early 1970s, the new technology that was to become known as computational fluid dynamics (CFD) began to emerge as a general tool for the analysis of fluid flow problems (see, for example, Gosman *et al*. 1969). The study of CFD ceased to be the esoteric concern of applied mathematicians and became accessible for application to practical engineering problems. This new methodology added a powerful theoretical capability to the engineer's armoury of dimensional analysis and integral and physical modelling then (and now) in widespread use to study the highly complex problems of the real world.

The study of fire behaviour inside buildings and other enclosures such as ships and aircraft was one such application. CFD provided the potential to study an extremely complicated problem that was only partly amenable to reduced-scale physical modelling because of the very large number of non-dimensional groups that needed to be preserved to simulate full-scale behaviour.

The starting point for the CFD models is the 'exact' system of coupled partial differential equations that describe the balance between the competing influences on mass, momentum, chemical species and energy within the fire and throughout the enclosure containing it. The solution of the 'exact' equations, resolving fully the length- and time-scales that occur in the flows associated with the turbulent combustion characteristic of fire, is still beyond the capabilities of even the largest computers currently available. As a consequence it is necessary to simplify this system of 'exact' equations by first time-averaging them and then solving the resulting continuous equations in discretized form over the domain of interest. The full rigour of the initial balance equations is now lost, to be replaced by uncertainties associated with the modelling of the turbulence and its interaction with the chemical kinetics and radiant heat transfer of the combustion process. Other uncertainties are also introduced as a result of the numerical approximations involved, but these will not be discussed in this paper. The author has recently reviewed these numerical aspects in the context of fire (Cox 1995), but such problems are shared with the much wider

CFD community as a whole, whereas those concerning the turbulence–chemistry–radiation interactions are more restricted to the particular nature of combustion systems in general and fire in particular. While there have been several excellent reviews of the treatments available for these phenomena in combustion systems (see, for example, Jones & Whitelaw 1982; Viskanta & Menguc 1987), they tend to say little concerning fire.

This paper gives a general overview of the progress that is being made in the modelling of fire by using CFD, emphasizing the 'fire science' rather than dwelling on the enabling numerical methodology. Inevitably, because of space limitations, detail is often sacrificed to ensure coverage of the breadth of this topic. It is hoped that the references cited are adequate to satisfy those wishing to probe deeper.

2. The principles

The effect of turbulence can be appreciated by inspection of the 'exact' instantaneous mass-continuity equation

$$\frac{\partial \rho}{\partial t} + \frac{\partial}{\partial x_j}(\rho u_j) = 0. \tag{2.1}$$

This simply states that the rate of accumulation of mass in an elementary control volume within the domain due to density changes balances the net rate of inflow across the volume boundaries.

Since both the density ρ and velocity u_j at a particular location x_j fluctuate due to the turbulence (see figure 1, which gives an indication of temperature fluctuations within a fire), a time mean equation can be written as

$$\frac{\partial \overline{\rho}}{\partial t} + \frac{\partial}{\partial x_j}(\overline{\rho u_j} + \overline{\rho' u_j'}) = 0, \tag{2.2}$$

where the instantaneous densities and velocities of equation (2.1) are broken down into time-mean and fluctuating components $\rho = \overline{\rho} + \rho'$ and $u_j = \overline{u}_j + u_j'$. Here, for example,

$$\overline{u}_j = \lim_{\Delta t \to \infty} \frac{1}{\Delta t} \int_{t_0}^{t_0 + \Delta t} u_j(t)\, \mathrm{d}t,$$

$$\overline{u_j'} \equiv 0.$$

In principle, the time mean is only statistically stationary if it is independent of t_0. In practice, fires grow and decay and the statistics are not strictly stationary. However, when time averages are taken over periods long enough to include many fluctuations (say tens of seconds), but shorter than the characteristic time-scale of the fire (minutes), it is possible to examine the gross non-stationary behaviour of fire.

From equation (2.2) it is apparent that, in addition to the 'expected' time-averaged form of equation (2.1), there is an extra term,

$$\frac{\partial}{\partial x_j}(\overline{\rho' u_j'}),$$

describing the transport of mass, due to the turbulent fluctuations in ρ and u_j. This term can take either sign depending upon the local behaviour of the density and velocity fields.

Similar substitutions and time-averaging of the more complex balance equations for momentum, energy and chemical species create many more complications and additional turbulent transport terms resulting from correlations between enthalpy, species concentrations and the components of velocity.

Using the density-weighted averaging, e.g.

$$u_j(t) = \tilde{u}_j + u_j'',$$

where

$$\tilde{u}_j = \overline{\rho u_j(t)}/\overline{\rho}$$

and

$$\overline{\rho u_j''} \equiv 0 \quad (\text{but } \overline{u_j''} \neq 0),$$

suggested by Favre (1965) for all variables, except density and pressure, for which conventional averaging is retained, the continuity equation then becomes

$$\frac{\partial \overline{\rho}}{\partial t} + \frac{\partial}{\partial x_j}(\overline{\rho}\tilde{u}_j) = 0, \tag{2.3}$$

and the remaining equations of conservation become:
momentum,

$$\frac{\partial}{\partial t}(\overline{\rho}\tilde{u}_i) + \frac{\partial}{\partial x_j}(\overline{\rho}\tilde{u}_j\tilde{u}_i) = -\frac{\partial \overline{p}}{\partial x_i} + \frac{\partial(\overline{\tau}_{ij} - \overline{\rho u_i'' u_j''})}{\partial x_j} + \overline{g}_i; \tag{2.4}$$

energy,

$$\frac{\partial}{\partial t}(\overline{\rho}\tilde{h}) + \frac{\partial}{\partial x_j}(\overline{\rho}\tilde{u}_j\tilde{h}) = \frac{\partial \overline{p}}{\partial t} + \frac{\partial}{\partial x_j}\left(\frac{k}{c_\mathrm{p}}\frac{\partial \overline{h}}{\partial x_j} - \overline{\rho u_j'' h''} - \overline{\dot{q}_j^\mathrm{R}}\right); \tag{2.5}$$

and species,

$$\frac{\partial}{\partial t}(\overline{\rho}\tilde{Y}_\alpha) + \frac{\partial}{\partial x_j}(\overline{\rho}\tilde{u}_j\tilde{Y}_\alpha) = \frac{\partial}{\partial x_j}\left(\overline{D\rho\frac{\partial Y_\alpha}{\partial x_j}} - \overline{\rho u_j'' Y_\alpha''}\right) + \overline{S}_\alpha, \tag{2.6}$$

where τ_{ij} is the viscous stress tensor, g_i is the body force term in the ith direction, k is the gas mixture thermal conductivity and $\dot{q}_j^\mathrm{R}$ is the radiative energy flux in the jth direction. Y_α is the mass fraction of species α, D is its molecular diffusion coefficient and S_α is the chemical source term describing the production or destruction of the species. The energy equation is expressed here in terms of the static enthalpy of the gas mixture

$$h = c_\mathrm{p}T + \sum_\alpha Y_\alpha H_\alpha,$$

where H_α is the heat of reaction of the species α and the specific heat of the mixture at constant pressure, c_p, is given by

$$c_\mathrm{p} = \sum_\alpha Y_\alpha c_{p,\alpha},$$

where $c_{p,\alpha}$ are the specific heats of the individual components.

In nearly all fire studies the unknown correlations are modelled with a 'buoyancy modified' version (Rodi 1978; Markatos *et al*. 1982) of the well-known k–ε model of turbulence, where

$$k \equiv \frac{1}{2}\frac{\overline{\rho u_i'' u_i''}}{\overline{\rho}}$$

is the kinetic energy of the turbulence and ε is the rate of its viscous dissipation. Here the shear stresses and scalar fluxes are first assumed, by analogy with kinetic gas theory, to be proportional to the local mean property gradients. The proportionality constant, a property of the flow rather than the fluid, is termed an eddy viscosity in the case of the shear stresses and an eddy diffusivity for the scalar fluxes, i.e.

$$\overline{\rho u_i'' u_j''} = \tfrac{2}{3}\delta_{ij}\left(\overline{\rho}k + \mu_t \frac{\partial \tilde{u}_k}{\partial x_k}\right) - \mu_t\left(\frac{\partial \tilde{u}_i}{\partial x_j} + \frac{\partial \tilde{u}_j}{\partial x_i}\right), \tag{2.7}$$

$$\overline{\rho u_j'' \phi''} = -\Gamma_\phi \frac{\partial \tilde{\phi}}{\partial x_j}. \tag{2.8}$$

Here ϕ is a general variable representing the species and enthalpy scalars.

The problem now concerns solving for the eddy viscosity μ_t and diffusivity Γ_ϕ. If the turbulent Schmidt and Prandtl numbers, σ_t, are assumed constant and it is assumed that

$$\Gamma_\phi = \mu_t/\sigma_t,$$

then these follow from the solution of two further transport equations for k and ε, with

$$\mu_t = C_\mu \overline{\rho} k^2/\varepsilon \tag{2.9}$$

where C_μ is assumed to be a 'constant' that has been determined from a substantial body of experimental studies of shear flow.

Implicit in this model of turbulence is the assumption that it is locally isotropic with μ_t and Γ_ϕ identical in all directions. This clearly is unlikely in flows under the influence of buoyancy. Instead current treatments (see, for example, Cox & Kumar 1987) account for the effects of buoyancy on turbulent mixing through the source terms in the balance equations for both k and ε. The effects of enhanced mixing in the unstably statified region above the fire source and of its inhibition in stably stratified ceiling layers are incorporated through the buoyancy production term

$$G_\mathrm{B} = -\beta g \frac{\mu_t}{\sigma_t}\frac{\partial \overline{T}}{\partial x_j}, \tag{2.10}$$

where the volumetric expansion coefficient

$$\beta = -\frac{1}{\overline{\rho}}\left(\frac{\partial \overline{\rho}}{\partial \overline{T}}\right)_p.$$

G_B takes either sign depending upon the local vertical temperature gradient.

Each of the conservation equations (2.3)–(2.6) and the balance equations for k and ε are now solved numerically, if the source terms can be closed, in the general form

$$\frac{\partial}{\partial t}(\overline{\rho}\tilde{\phi}) + \frac{\partial}{\partial x_j}(\overline{\rho}\tilde{u}_j\tilde{\phi}) = \frac{\partial}{\partial x_j}\left(\Gamma_\phi \frac{\partial \tilde{\phi}}{\partial x_j}\right) + \overline{S}_\phi, \tag{2.11}$$

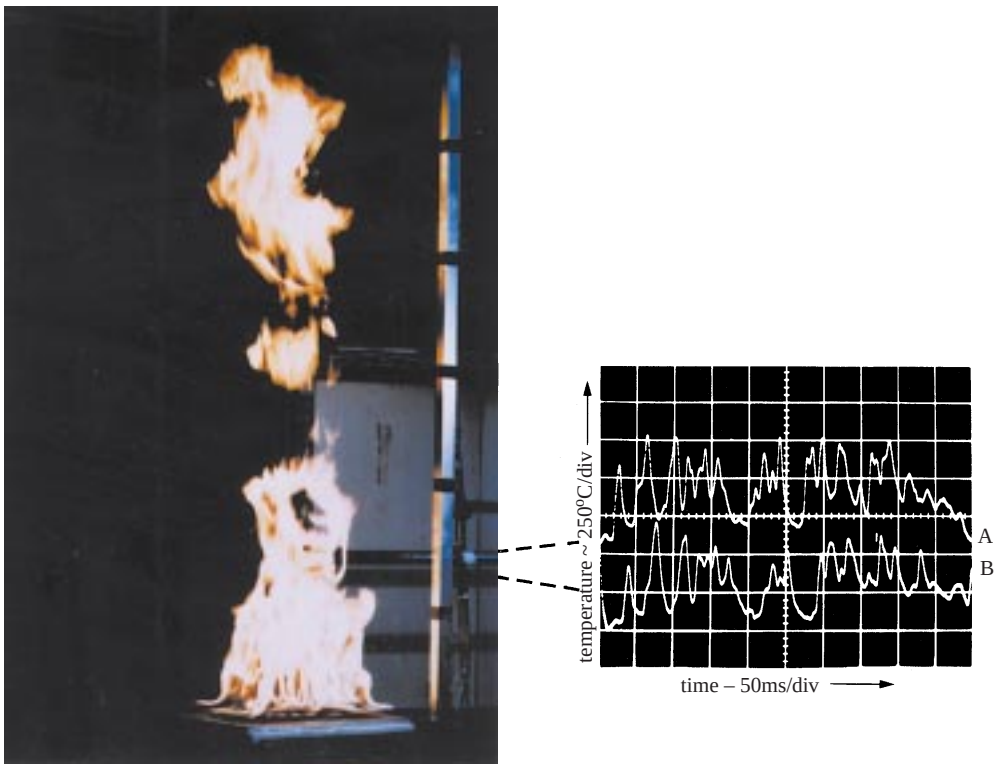

Figure 1. Temperature fluctuations measured by two fine-wire thermocouples 50 mm apart.

where ϕ is a generic (Favre-averaged) property of the fluid, S_ϕ is a source term and Γ_ϕ is an exchange coefficient appropriate to ϕ.

Γ_ϕ is obtained from solutions of equation (2.11) when $\phi = k$ and $\phi = \varepsilon$. The enthalpy and species conservation equations are represented by this equation when $\phi = h$ and $\phi = Y_\alpha$, respectively. Pressure is determined from a pressure correction equation deduced from the mass conservation equation (when $\phi = 1$) and the momentum equations (when $\phi = u_j$).

3. Chemical and enthalpy source closure

Our major concern now is to close the species and enthalpy source terms. The closures need to be acceptably accurate to describe the processes peculiar to fire. The effects of buoyancy on turbulent transport have already been discussed but we now need to consider the effects of fluctuations on chemical kinetics, $(\overline{S}_\alpha)$, and radiant heat transfer $(\overline{\dot{q}_j^{\mathrm{R}}})$. Since both processes are highly nonlinear in temperature, fluctuations can cause greatly enhanced levels of mean reaction rate and mean radiant heat flux.

If the reaction mechanism can be reduced to a single global one-step reaction,

$$\mathrm{F} + r \cdot \mathrm{O} \xrightarrow{k} (1 + r)\mathrm{P},$$

i.e. unit mass of fuel reacts with its stoichiometric mass requirement, r, of oxidizer to provide $(1 + r)$ mass units of product, then a simple Arrhenius expression describing

the instantaneous rate constant for the reaction can be written

$$k = B \exp\left(-\frac{T_\alpha}{T}\right), \tag{3.1}$$

where B is the pre-exponential factor for the reaction and T_α is its activation temperature. On replacing T by its mean and fluctuating components and time-averaging, this becomes

$$\overline{k} = B \exp\left(-\frac{T_\alpha}{\overline{T}}\right)\left(1 + \overline{T'^2}\left(\frac{T_\alpha^2}{2\overline{T}^4} - \frac{T_\alpha}{\overline{T}^3}\right) + \dots\right). \tag{3.2}$$

The simple substitution of mean temperature into equation (3.1) would clearly be misleading. Evidently the mean reaction rate can be substantially higher than a rate based upon consideration only of laminar chemistry. Moss (1995) provides an illustration of the magnitude of the difference for a fluctuation pattern assumed to be a square wave. For a reaction with an activation temperature of 20 000 K and reactant and product temperatures of 500 and 2000 K, respectively, the turbulent rate exceeds the laminar by a factor of 200!

A similar analysis (Cox 1977) for the time-mean radiant intensity received at a surface from a flame whose temperature, T, and emissivity, ε, fluctuate but whose view factor, ω, does not gives

$$\overline{I} = \sigma\omega\overline{\varepsilon}\overline{T}^4\left(1 + 6\frac{\overline{T'^2}}{\overline{T}^2} + \frac{\overline{T'^4}}{\overline{T}^4} + 4\frac{\overline{\varepsilon' T'}}{\overline{\varepsilon}\,\overline{T}} + 4\frac{\overline{\varepsilon' T'^3}}{\overline{\varepsilon}\overline{T}^3} \dots\right). \tag{3.3}$$

This suggests that for a temperature intensity of fluctuation, $(\overline{T'^2}/\overline{T})^{1/2}$ greater than about 40%, the additional terms will exceed the first term that would have been expected from consideration of mean properties alone. Such fluctuation intensities are quite likely in the flame systems under consideration (see, for example, Cox & Chitty 1982).

(*a*) *Eddy break-up combustion model*

In the turbulent diffusion flame systems characteristic of fire, most chemical reactions can be considered fast compared to the comparatively slow physical mixing of fuel with oxidizer. To determine this mixing rate, the eddy break-up model, originally proposed by Spalding (1971) for the treatment of premixed flames, is often exploited. Spalding argued that the rate of reaction in such systems was determined by the intermingling, at microscale level, of fragments of unburnt reactants with hot product. This breaking and intermingling would be driven by local turbulent strain rates until, at the smallest scales, viscous forces became dominant. Spalding assumed that the rate of reaction was thus equal to the rate of dissipation of turbulent kinetic energy at this small scale. Applying this model to the non-premixed flame gives, for example,

$$\overline{S}_\mathrm{f} = -C_\mathrm{ebu}\overline{\rho}\frac{\varepsilon}{k}(\overline{Y_\mathrm{f}'^2})^{1/2}, \tag{3.4}$$

where $\overline{Y_\mathrm{f}'^2}$ is the variance in fluctuations of the fuel mass fraction obtained from a further balance equation of the form of equation (2.11) and $C_\mathrm{ebu}/Y_\mathrm{f}'^2$ is a constant. This was later modified by Magnussen & Hjertager (1976) for diffusion flames by

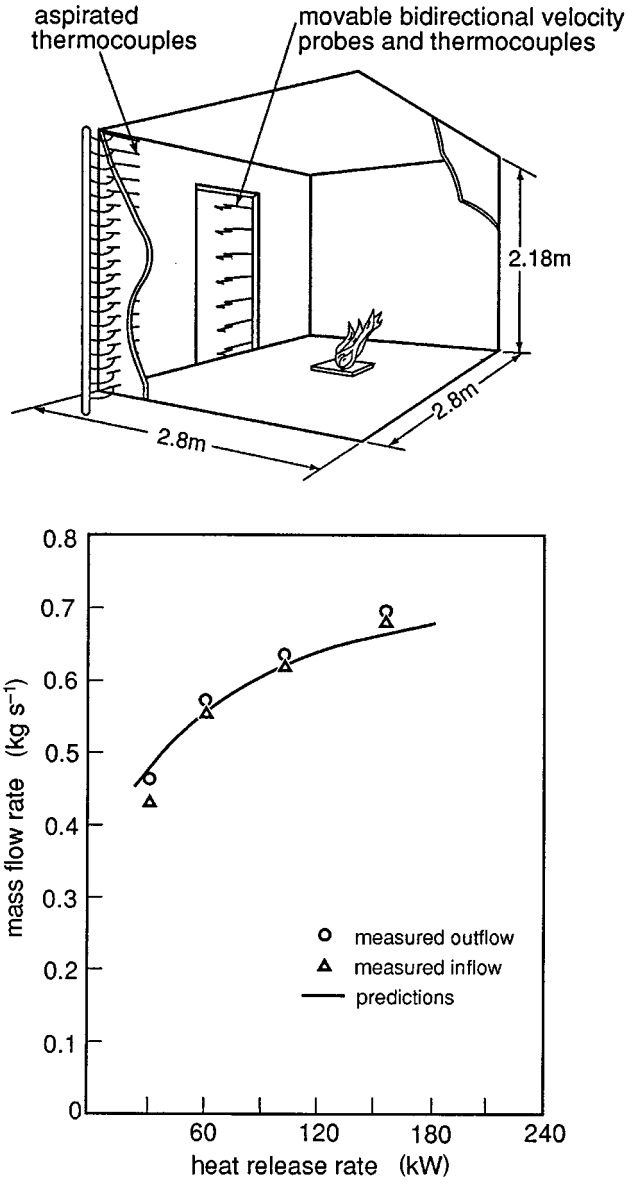

Figure 2. Schematic diagram of room fire experiments and predictions of doorway mass flow rates.

assuming that it is proportional to the mean mass fraction and that the rate of reaction is further controlled by the deficient reactant:

$$\overline{S}_{\mathrm{f}} = -C_{\mathrm{ebu}}\overline{\rho}\frac{\varepsilon}{k}\min\left\{\overline{Y}_{\mathrm{f}}, \frac{\overline{Y}_{\mathrm{o}}}{r}\right\}. \tag{3.5}$$

Thus rate control will switch from oxidizer close to the fire to fuel remote from it. This allows the local rate of fuel consumption and product generation to be

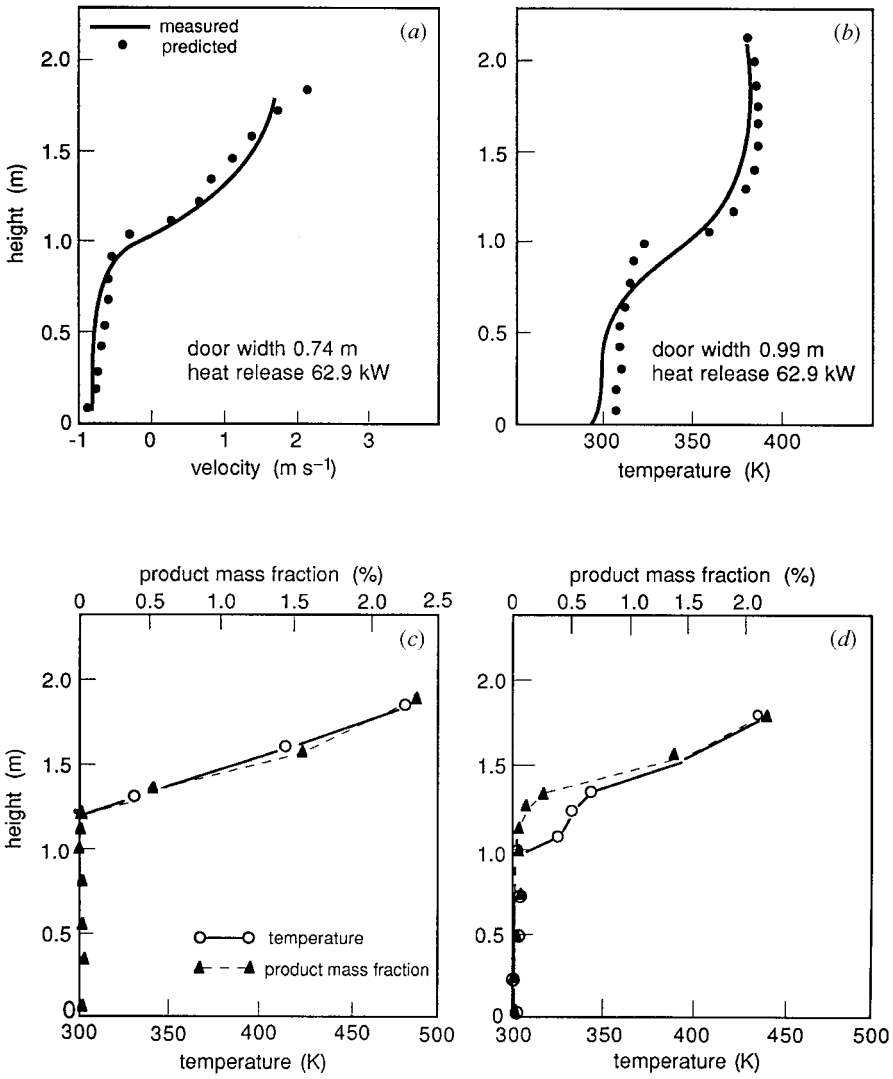

Figure 3. Measured and predicted gas velocities (a) and temperatures (b) on doorway centreline for central 63 kW fire; (c) and (d) show predicted gas temperatures and product mass fractions with and without thermal radiation for a corner fire ((c) no radiation model; (d) six-flux radiation model).

determined without the need to probe deeply into the detailed kinetics involved. The combustion products can be assumed to be CO_2 and H_2O in their stoichiometric proportions. The model therefore is of considerable value in determining the volume in which the combustion and heat release processes take place but does not address issues associated with finite rate kinetics. Although the chemistry can be considered to be fast for the primary heat releasing reactions, the formation and burnout of CO and soot are slower, and more comparable with turbulent mixing rates. Of course it is these reactions which are so important for the establishment of the toxicity hazard of fire gases and, through flame emissivities, radiant heat emissions.

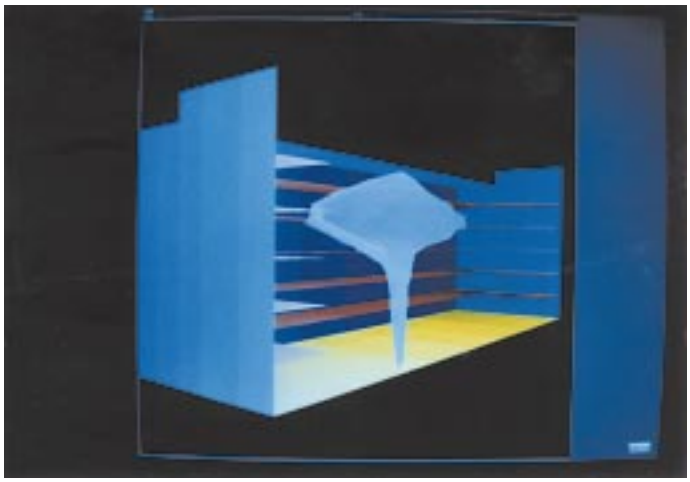

Figure 4. Field model prediction of smoke rise in an atrium against an ambient temperature gradient.

However, two examples are shown here to illustrate the application of models employing this simple type of fast chemistry closure. The first concerns comparisons between experiments and predictions for gas-burner fire simulations in a domestic sized room. Comparisons of this kind are of course essential to establish confidence in, and verification of, the methodology. Figure 2 shows the experimental arrangement together with predictions and measurements of integrated mass fluxes in and out of the doorway for fires of a range of heat release rates. Figure 3*a*, *b* compares measured with predicted velocities and gas temperatures on the centreline of the doorway for a fire of heat release rate 63 kW situated in the centre of the room. As can be seen, predictions are in reasonable agreement with the measured data. Perhaps the most interesting result from the research viewpoint is the difference, for a corner fire, in the predicted vertical temperature and product mass fraction profiles as calculated with and without radiant heat transfer in the model (figure 3*c*, *d*). These suggest that the 'bump' in the measured temperature profile at the bottom of the smoke layer results from radiantly heated air rising from cooler surfaces below the smoke rather than the products of combustion. This heated air constitutes 25% of the total outflow from the room. This additional outflow may or may not have practical implications for smoke control problems but it is clear that it would be very difficult to obtain this information any other way.

The second example concerns a 'practical' engineering evaluation of the smoke control measures that were proposed for the redevelopment of Battersea Power Station as an indoor 'leisure park' (Cox *et al*. 1990). Modelling was conducted of the consequences of fire occurring in various locations within a single atrium enclosure occupying the original generating hall. Because of the exceptionally large volume of this atrium (nearly half a million cubic metres overall), containing public galleries opening on to it, there was little guidance on how to design smoke control systems to protect the occupants in the event of fire. Traditional advice starts with the assumption that smoke rises to the top of such a volume and fills it from the top down. The CFD calculations suggested (figure 4) that such an assumption could not necessarily be made for such a large volume where a temperature gradient will develop between

floor and ceiling due to ambient heating. The analysis permitted a smoke control strategy to be devised which did not rely on such an assumption.

Based upon the successes of simulations of this kind in a wide variety of enclosure types, CFD has become increasingly employed in both 'forensic' and design environments for the study of problems associated mainly with the movement of smoke. Recent examples include the public enquiries into the fire disasters in the Kings Cross Underground Railway Station and on the Scandinavian Star passenger ferry. Examples of application to design include the Lloyds Building in the City of London, the Tokyo Dome sports stadium and the Channel Tunnel vehicle shuttle wagons.

(*b*) *Laminar flamelet combustion model*

The incorporation of complex combustion chemistry into the closure scheme by making not only the fast chemistry assumption but also by further assuming that the local instantaneous composition and temperature within the turbulent flame is the same as that in a steady laminar diffusion flame has been particularly popular for the treatment of a number of non-premixed systems. The species conservation equation can be conveniently recast in terms of a conserved scalar, ξ, the mixture fraction,

$$\xi = \frac{\beta - \beta_{\mathrm{o}}}{\beta_{\mathrm{f}} - \beta_{\mathrm{o}}}, \tag{3.6}$$

as

$$\frac{\partial}{\partial t}(\overline{\rho}\tilde{\xi}) + \frac{\partial}{\partial x_j}(\overline{\rho}\tilde{u}_j\tilde{\xi}) - \frac{\partial}{\partial x_j}\left(\Gamma_\xi \frac{\partial \tilde{\xi}}{\partial x_j}\right) = 0, \tag{3.7}$$

where $\beta \equiv Y_{\mathrm{f}} - (Y_{\mathrm{o}}/r)$ and the subscripts 'f' and 'o' refer to fuel and oxidizer, respectively. ξ takes the value of unity in the fuel stream and zero in the oxidizer.

Since this equation contains no source term it side-steps the problem of turbulent closure. Instead all influences of turbulence on the kinetics are embedded within the behaviour of ξ. Equation (3.6) can be solved for the mean mixture fraction, $\tilde{\xi}$, in much the same way as equation (2.11) is solved for $\tilde{\phi}$, since it is subject to the same transport processes of convection and diffusion. The outstanding problem is then to relate the instantaneous species mass fractions, Y_α, to the instantaneous behaviour of ξ and to find a way to relate these instantaneous relationships to their time-mean values.

By making the assumption that the relationship between Y_α and ξ is locally the same in the turbulent flame as it is in a laminar flame, then the first of these problems is resolved since the kinetics of laminar flames can be modelled theoretically for many of the simpler fuels (e.g. methane, methanol and propane). For the more complex types of fuel of more practical concern in fire situations, the appropriate information needs to be obtained from experimental measurements on laminar flames representative of them.

Detailed libraries of composition-mixture fraction data can thus be generated for use in post-processing the results of predictions for the hydrodynamic flow field—assuming that the resulting species concentration field does not significantly influence the local buoyancy forces. In the fuel-lean region of the flamelet, the major gas species (O_2, N_2, CO_2, H_2O) can be reasonably well described by thermodynamic equilibrium. This is not so for CO, nor is it for the major species in the fuel-rich region. However,

Sivathanu & Faeth (1990*a*) have shown acceptably universal experimentally derived state relationships across the whole range of flamelet conditions in hydrocarbon–air flames that can be employed in conjunction with the 'laminar flamelet' concept.

Work is also currently underway to establish similar relationships for polymeric fuels more likely to be of concern in 'real world' applications. Initial studies involve gaseous propylene and prevapourized methylmethacrylate, representing the 'monomer' decomposition products of polypropylene and polymethylmethacrylate.

With this information the mean species mass fractions can be determined from a knowledge of the statistical character of the fluctuating property field, i.e.

$$\tilde{Y}_\alpha = \int_0^1 Y_\alpha(\xi) P(\xi)\, \mathrm{d}\xi, \tag{3.8}$$

where $P(\xi)$ is the probability density function (PDF) describing mixture fraction fluctuations. In engineering applications it has been common to assume, *a priori*, a functional form for $P(\xi)$ although there are more sophisticated approaches where the PDF is determined directly, but these have yet to be applied to fire problems. The detail of the assumed PDF is determined by its first two moments, $\tilde{\xi}$ and $\tilde{\xi}''^2$. These are obtained from solution of two further equations of the form of equation (2.11). A beta-function form for $P(\xi)$ has been found to be both economical and reasonably representative of the mixing involved. While results for higher momentum flame systems have been shown to be relatively insensitive to the precise shape of the PDF, there is still some uncertainty as to whether this is so for buoyant fires. Figure 5 illustrates comparisons between predictions using a beta function (Syed 1990) and measurements for an unbounded 28 kW methane fire simulation on a 0.3 m^2 burner. The agreement between predicted and measured mean-mass fractions of the gas species can be seen to be reasonably good.

The calculation was initiated with boundary conditions measured in the turbulent flow 0.14 m above the fuel bed. This was to overcome difficulties associated with modelling the laminar-turbulent transition that occurs below this point and immediately above the fuel bed. This problem is not particularly critical for calculation of smoke movement in the far field but does become so for modelling details of the buoyant flame itself.

The 'laminar flamelet' modelling of the combustion within non-premixed flames has been fairly successful for predicting conditions in various flame systems, most notably, from the fire point of view, by reproducing realistically lower levels of CO than would result from a prediction assuming thermodynamic equilibrium. However, in conditions where the fire is at its most dangerous in terms of its toxicity, when the oxidizer contains a substantial proportion of combustion products instead of fresh air, then the fast chemistry assumption is most likely to fail. Low temperatures will lead to reduced reaction rates and the assumption of mixing control will break down. There is currently insufficient evidence to determine how serious this is for the modelling of poorly ventilated fires. Clearly, this is an area which requires particular attention.

Bilger (1993) has proposed a 'conditional moment' closure model which offers a solution for the prediction of finite-rate kinetics by using conditionally averaging quantities to achieve closure of the chemical production terms. Typically, the species mass fraction, Y_α, is averaged conditionally on fixed values of mixture fraction, ξ. This approach, which has been demonstrated to accurately predict the finite-rate kinetics

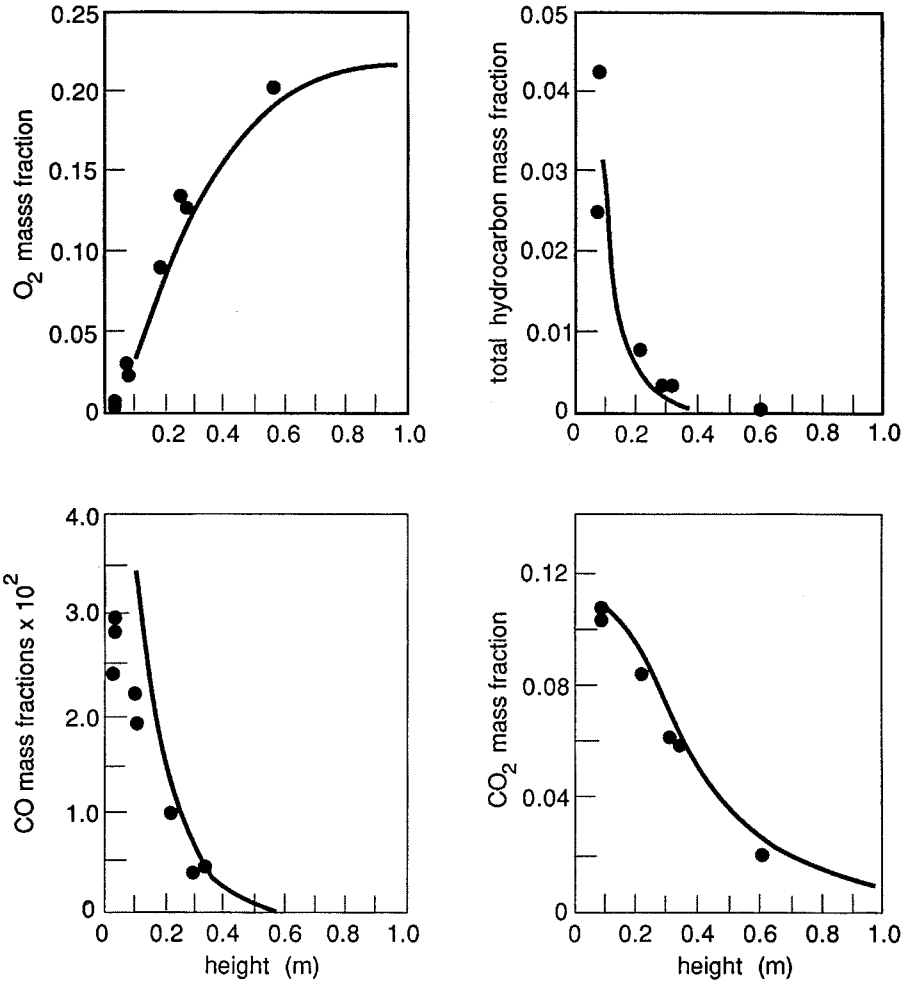

Figure 5. Laminar flamelet calculations and measurements (shown by dots) on axis of 28 kW methane fire simulation (Syed 1990).

of turbulent hydrogen jet flames (Smith *et al*. 1992) but has yet to be applied to fire, looks promising although expensive for engineering application. Until such a time as models of this kind have been developed and proven, it is necessary instead to use experimental correlations for product emissions as functions of the rate of fuel gasification obtained from bench-scale tests and large-scale fires. Information of this kind is available, in abundance, for well ventilated fires but to a lesser degree for 'underventilated' fires (see, for example, Tewarson *et al*. 1981).

(*c*) *Soot*

The soot generated by fire contributes critically to both the respirable and obscurational hazards of smoke as well as to the emissivity of flame and therefore its propensity to radiate heat back to its own fuel and to the, as yet, uninvolved fuel nearby. Soot is formed in large concentrations in most fires, reflecting the relatively

inefficient fuel–air mixing processes involved which permit high-temperature fuel-rich regions to persist for long times. Radiant heat losses from the soot particulates to the surroundings effectively freeze the kinetics, denying oxidation and burnout of the soot and thus causing the large volumes of smoke characteristic of fires.

The processes of soot formation and destruction are extremely complex. Experimental studies with laminar diffusion flames show that soot is generated in a very narrow zone on the fuel-rich side of the stoichiometric contour and is destroyed by oxidation in oxygen-rich regions. Clearly, in a turbulent flame similar difficulties arise in the modelling of these phenomena, as were described previously for gaseous species. However, the physical and chemical time-scales characteristic of soot formation and oxidation are long in comparison with those associated with the gaseous species and thus such simple state relationships as those described above are not available. Measurements show that the state relationships for soot are functions of the 'residence time' of the fuel in the flame and thus soot volume fractions increase, in mixture fraction space, with travel distance from the fuel bed. Although near universal state relationships have been shown to be valid in the regions beyond the flame tip (Sivathanu & Faeth 1990*b*), the use of the laminar flamelet methodology within the flame becomes very complex.

A more pragmatic approach, somewhat similar to the eddy-break-up model for the gas phase, using only time-mean property fields was used by Malalasekera (1988) with ideas proposed by Magnussen & Hjertager (1976). He solved a transport equation for mean soot mass fraction, $\overline{Y}_\mathrm{s}$, of the form of equation (2.11), where the source term comprises two components for soot formation and soot burnout:

$$S_\mathrm{s} = S_\mathrm{f} - S_\mathrm{b}. \tag{3.9}$$

Soot formation, S_f, was modelled after Khan & Greeves (1974) as a simplified global one-step reaction combining the effects of pyrolysis, nucleation, surface growth, coagulation and agglomeration:

$$S_\mathrm{f} = C_\mathrm{f} p_\mathrm{f} \psi^3 \exp\left(-\frac{E_\mathrm{f}}{RT}\right). \tag{3.10}$$

Soot burnout, S_b, was controlled by the slower of the two rates of oxidation (Lee *et al*. 1962) and the physical mixing of soot with oxidizer was again controlled by the deficient reactant:

$$S_\mathrm{b} = \min\left\{C_\mathrm{b} Y_\mathrm{s} \frac{p_\mathrm{o}}{T^{1/2}} \exp\left(-\frac{E}{RT}\right), C_\mathrm{ebu}\rho\frac{\varepsilon}{k} Y_\mathrm{s}, C_\mathrm{ebu}\rho\frac{\varepsilon}{k}\frac{Y_\mathrm{o}}{r_\mathrm{s}}\left(\frac{Y_\mathrm{s} r_\mathrm{s}}{Y_\mathrm{s} r_\mathrm{s} + Y_\mathrm{f} r}\right)\right\}, \tag{3.11}$$

where C_f and C_b are model constants, p_f and p_o are the partial pressures of fuel and oxidizer, respectively, and ψ is the local equivalence ratio.

This greatly simplifies the processes involved, ignoring the detailed influences of turbulence on soot formation and oxidation. However, Malalasekera was able to show (figure 6) a good agreement between predictions and the measurements of Modak & Croce (1977) for mass burning rates of square samples of polymethylmethacrylate of varying area.

An even simpler global assumption is often of considerable assistance in undertaking practical engineering estimates, particularly of thermal radiation. Markstein (1984) observed that the well-known constancy of the fraction of total heat release rate lost by radiation in buoyant diffusion flames of height-to-base ratio greater than

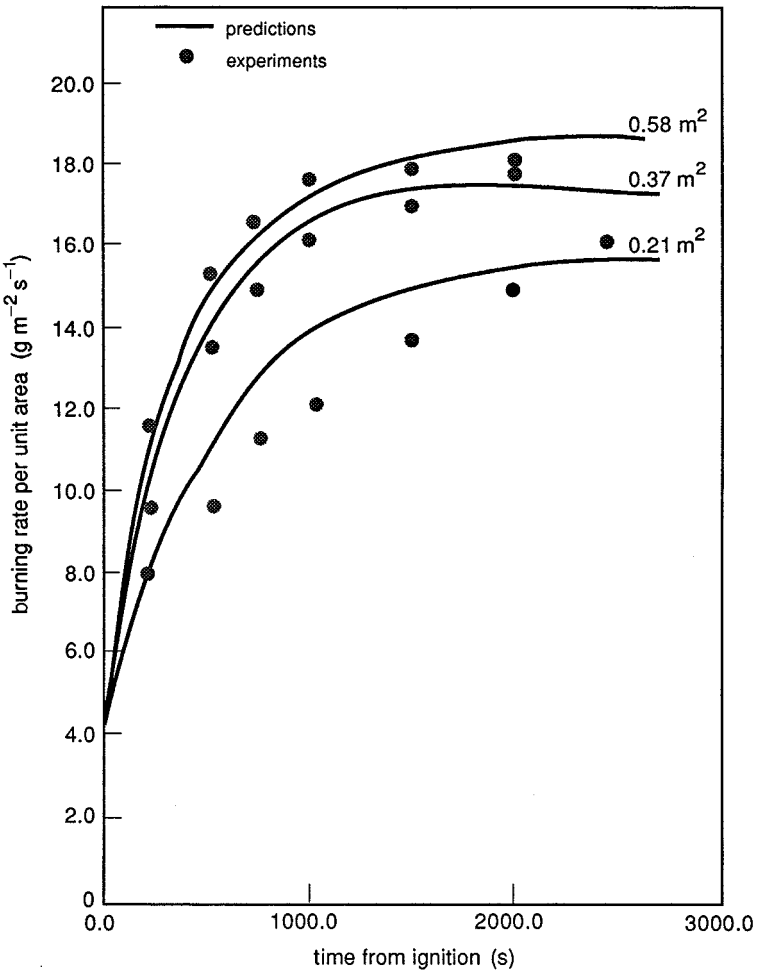

Figure 6. Comparison of predicted and measured transient burning rates for PMMA fires of different pool areas (Malalasekera 1988).

one, is well correlated by laminar 'smoke point' measurements. For flames at their smoke point the competing mechanisms of soot formation and oxidation are in balance. The radiated fraction ranges from about 18% for methane to around 50% for acetylene. It was also established that the rate of release of the incomplete products of combustion (i.e. soot, tars, etc.) was similarly correlated, ranging from close to zero for methane to around 30% for polystyrene and ethylene. These observations allow the effects in the far field of radiant heat loss and incomplete combustion to be accounted for, at least for well-ventilated fires.

(*d*) *Thermal radiation*

Radiation is usually the dominant mode of heat transfer in fires of any size. It is this which provides the heat of gasification necessary to liberate fuel volatiles from the condensed phase which on reaction with the oxygen in the entrained air releases further heat to maintain and further enhance the process. Continuous luminous radi-

ation from soot particulates and banded gaseous emissions from the product gases contribute to this energy transfer. It enters the transport equation set only as a source term in the energy conservation equation (2.5). This term is obtained from approximations to the radiative transfer equation. The spectral radiation intensity, I_λ, along a path of length, s, of a monochromatic pencil of 'rays' of wavelength λ passing through an elementary control volume in the direction Ω is

$$\frac{\partial I_\lambda}{\partial s} = -(a_\lambda + s_\lambda)I_\lambda + a_\lambda I_{\mathrm{b},\lambda} + \frac{s_\lambda}{4\pi}\int_{\Omega'=0}^{4\pi} I_\lambda \,\mathrm{d}\Omega', \tag{3.12}$$

where a_λ and s_λ are spectral absorption and scattering coefficients, respectively; $I_{\mathrm{b},\lambda}$ is the spectral intensity of black body emission from within the volume. To determine the local contribution to the energy conservation equation, this needs to be integrated over all wavelengths and directions for each hydrodynamic control volume. Several approximate methods have been devised for this purpose and have been incorporated in simulations of fire (see, for example, Cox 1995).

The difficulty of predicting radiant heat transfer from a fluctuating medium has already been illustrated by the example given by equation (3.2) and the preceding discussion concerning soot. Again, both pragmatic and scientifically more rigorous approaches can be adopted. Most practical calculations totally ignore the effects of turbulent fluctuations in the scalar property fields and couple a calculation based on time-mean properties to the turbulent flow-field calculation. By using either flux methods or the discrete transfer model to solve the radiative transfer equation, reasonable agreement can be demonstrated for predictions of the radiant heat flux to the walls of enclosure fires at least remote from the fire itself.

For the fire source, laminar flamelet modelling studies have confirmed the qualitative features of equation (3.2). Faeth *et al.* (1985), for example, have shown for a non-sooting hydrogen–air jet diffusion flame a doubling of the predicted radiation intensities calculated by using only time-mean values due to turbulence-radiation fluctuations. Their laminar flamelet predictions were within 30% of measurements, tending to overestimate intensities. In studies of buoyant methane fire simulations, using a two-step model for nucleation and growth for soot formation and a simple model for residence times, Syed (1990) showed similar trends (figure 7), somewhat overpredicting measured intensities of the non-luminous infrared radiation but accurately predicting the visible and near infrared components of the continuous soot emissions.

4. Solid-phase combustion

CFD has an important role to play in the prediction of the 'reaction to fire' of solid combustibles. This is a particularly important area of fire-safety science since it is central to the issue of the propagation of fire within enclosures. The physical orientation of a solid combustible will influence its rate of gasification under fire conditions. For example, flames will spread much more rapidly upwards over a specimen of solid 'fuel' mounted vertically than over that same specimen when mounted horizontally. The area of fuel thus involved in pyrolysis is determined by the response of the solid to heat transfer from the gas phase.

The behaviour of the solid combustibles can be described by again applying the conservation principles within the bulk of the solid, subject to the boundary conditions set by the gas phase. For a porous solid, the mass continuity and energy

PHILOSOPHICAL TRANSACTIONS OF THE ROYAL SOCIETY A MATHEMATICAL, PHYSICAL & ENGINEERING SCIENCES

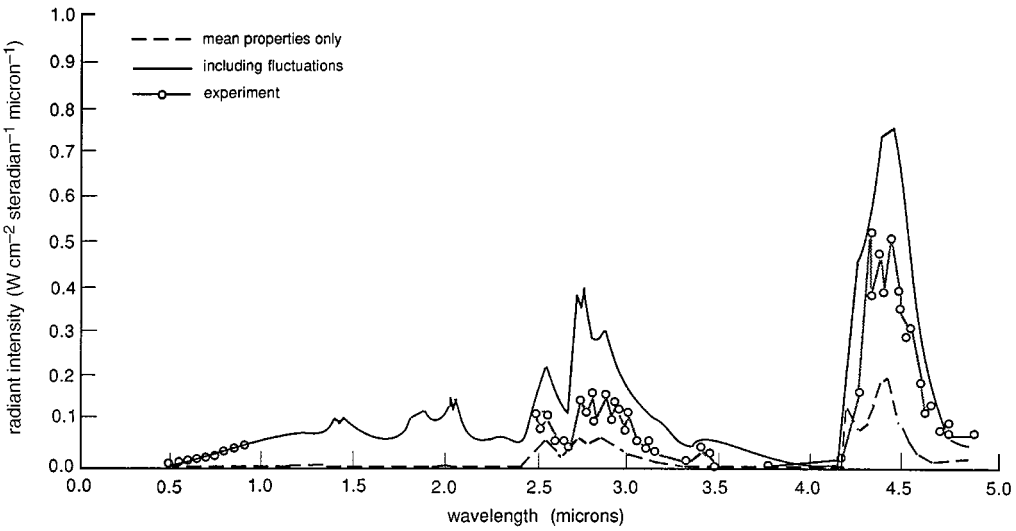

Figure 7. Predicted and measured spectral radiant intensity along a horizontal line of sight 0.45 m above a 28 kW methane fire simulation (Syed 1990).

conservation equations will often be sufficient if the solid can be assumed to offer no resistance to the flow of the gaseous pyrolysates from within its bulk.

Then the mass continuity equation is

$$\frac{\partial \rho_{\mathrm{s}}}{\partial t} + \frac{\partial}{\partial x_j}(\rho u_j) = 0, \tag{4.1}$$

where ρ_{s} is the instantaneous local density of the solid, and the energy conservation equation is

$$\frac{\partial}{\partial t}(\rho_{\mathrm{s}} c_{\mathrm{s}} T_{\mathrm{s}}) + \frac{\partial}{\partial x_j}(\rho u_j c_{\mathrm{p}} T_{\mathrm{s}}) = \frac{\partial}{\partial x_j}\left(k_{\mathrm{s}} \frac{\partial T_{\mathrm{s}}}{\partial x_j} - \dot{q}^{\mathrm{R}}\right) - H_{\mathrm{p}} \frac{\partial \rho_{\mathrm{s}}}{\partial t}, \tag{4.2}$$

where H_{p} is the endothermic heat of pyrolysis. The terms on the left-hand side of equation (4.2) represent the unsteady accumulation of energy in the solid together with the energy carried by the gas pyrolysates through the elementary control volume. The right-hand side comprises terms describing thermal conduction, the influence of in-depth absorption of thermal radiation and the energy lost in the phase change. An Arrhenius pyrolysis rate equation closes the system of equations:

$$\frac{\partial \rho_{\mathrm{s}}}{\partial t} = -B \rho_{\mathrm{s}} \exp\left(\frac{T_{\mathrm{a}}}{T_{\mathrm{s}}}\right). \tag{4.3}$$

These equations can now be solved subject to the boundary condition at the solid surface that

$$\dot{q}''_{\mathrm{net}} = -k \frac{\partial T}{\partial x_j}, \tag{4.4}$$

where $\dot{q}''_{\mathrm{net}}$ represents the net heat transfer to the solid from the gas phase.

Extensive studies of this kind have been conducted by di Blasi *et al.* (1988) for well-behaved materials such as polymethylmethacrylate and to a lesser degree wood, but for many situations involving the kind of realistic furnishing and lining materials

to be found in comfortable surroundings such as buildings and transport vehicles, a rigorous analysis such as this is not a practical proposition. Physical effects such as delamination, cracking and bubbling are not readily amenable to such a treatment and a more pragmatic approach needs to be adopted. A new family of reaction-to-fire bench-scale test methods developed with this purpose in mind is evolving which permits a full coupling between gas and solid phases to be made, exploiting test data obtained under standardized conditions.

This work is still in its infancy but figure 8 illustrates some recent predictions obtained from such an approach by Zhenghua Yan and the author for the heat released through an opening from a room lined with timber 'particle board'. The CFD modelling of heat transfer from a 100 kW gas burner fire to the room linings has been coupled to bench-scale test data, obtained from a 'cone calorimeter', for lining fuel mass release as a function of imposed heat flux. This calorimeter (see Babrauskas 1992) provides heat and mass evolution rates from 0.1 m×0.1 m specimens of material at various levels of incident heat exposure. In the example illustrated, the test data for imposed fluxes of 25 and 50 have been approximated by a single curve (figure 8*b*) relating 'fuel' mass release rate with time. For simplicity, in this preliminary study, the fuel has been assumed to be methane, which is evolved from the lining once the surface temperature of the elemental area of timber particle board exceeds a critical ignition temperature, here taken as 450 °C.

5. Conclusions

CFD is now widely recognized for its vital role in both fire-safety science and fire-safety engineering. This has taken longer than in many other areas of engineering science, partly because of the complexity of the topic but also because of an understandable inertia in embracing novel methods in a field which has a direct bearing on life safety and where it is often felt prudent to 'leave well alone'.

The degree to which sophistication is required in the submodels that describe the influences of turbulence on reaction kinetics and radiant heat transfer depends on the particular application. For many problems associated with the movement of smoke, the greater complexity of the laminar flamelet and more sophisticated closures is not required. If, in these applications, estimates of local CO concentrations are needed then either the eddy-break-up model with reduced chemical schemes or simple experimentally derived source terms can be exploited. However, if a faithful prediction is required for conditions where the air supply to the fire is vitiated by its own combustion products then more advanced models are necessary.

Similar conclusions can be drawn for gas-phase heat transfer and condensed-phase combustion. While very detailed solutions can be obtained for the gasification of pure homogeneous materials such as polymethylmethacrylate, these will, unfortunately, be of little value when applied to practical building linings or contents which are often composites which char, melt, crack and delaminate under fire conditions. For the treatment of these, 'test-based' approaches need to be coupled to CFD calculations for the gas phase. It is only CFD that is sufficiently general to be able to calculate heat transfer in the wide range of geometrical scenarios of the real world. The coupling of gas-phase CFD calculations to the response of solid-phase combustibles that are to be found in furnished buildings or transport vehicles remains a very important area

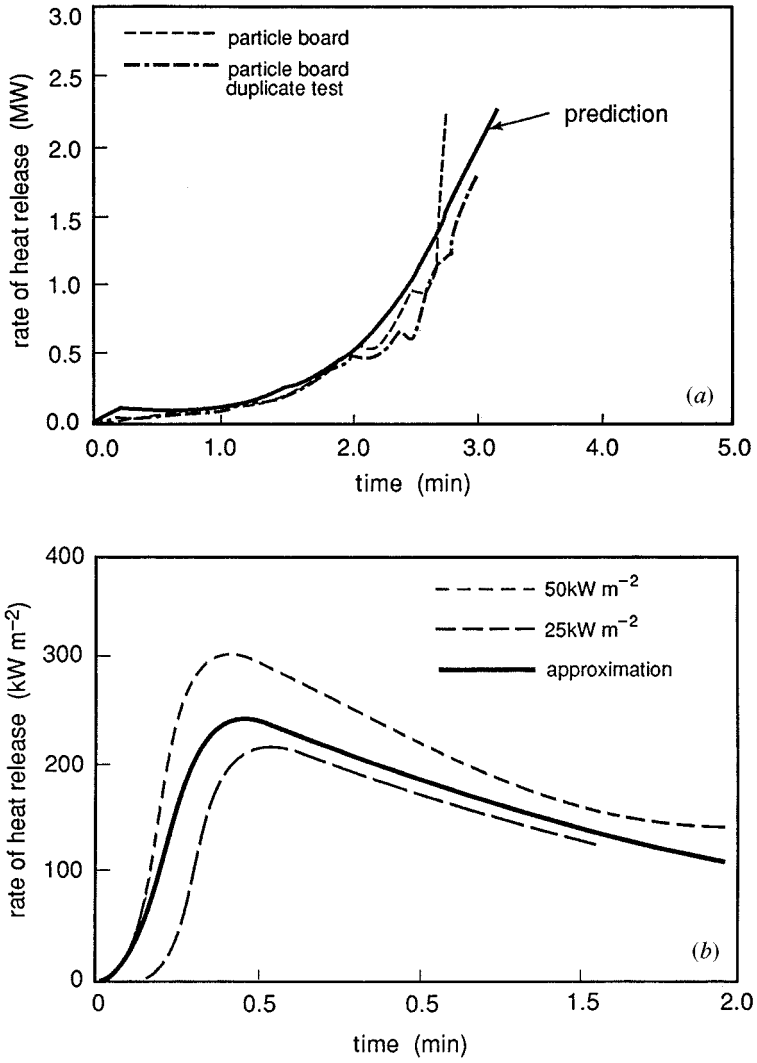

Figure 8. (*a*) Predicted and measured heat release rate for timer 'particle board' in a small room. (*b*) Heat release rate for 0.1 m × 0.1 m sample of timber 'particle board' in cone calorimeter

of application which should help deliver a more robust 'standardized' fire-testing regime for their selection and control.

There are still many areas of CFD that require development and improvement, particularly in the treatment of buoyant flows characteristic of fire. Turbulence modelling will improve as second-moment closures eventually replace k–ε models in engineering application. Large eddy and direct numerical simulations will provide insights into the underlying physics involved. More faithful representation of chemical kinetics will be incorporable as computer hardware continues to evolve at ever increasing pace. In the author's laboratory the number of numerical control volumes now being used to study fire problems is five hundred times greater than in the late 1970s, reflecting the substantial improvements in both computer speed and memory over the period.

The scientific developments will occur encouraged by the continuing improvements in hardware. The resulting tools will become more accessible to the practitioner through computer-aided design man–machine interfaces. It will be for the profession of Fire Safety Engineering to determine how it can use these new tools to achieve safe and cost effective design.

Reproduced by permission of the Building Research Establishment Ltd.

References

Babrauskus, V. 1992 The cone calorimeter. In *Heat release in fires* (ed. V. Babrausas & S. J. Grayson), pp. 61–91. New York: Elsevier.

Bilger, R. W. 1993 Conditional moment closure for turbulent reacting flow. *Phys. Fluids* A **5**, 436–444.

Cox, G. 1977 On radiant heat transfer from turbulent flames. *Combust. Sci. Tech.* **17**, 75–78.

Cox, G. 1995 Compartment fire modelling. In *Combustion fundamentals of fire* (ed. G. Cox), pp. 329–404. London: Academic.

Cox, G. & Chitty, R. 1982 Some stochastic properties of fire plumes. *Fire Mater.* **6**, 127–134.

Cox, G. & Kumar, S. 1987 Field modelling of fire in forced ventilated enclosures. *Combust. Sci. Tech.* **52**, 7–23.

Cox, G., Kumar, S., Cumber, P., Thomson, V. & Porter, A. 1990 Fire simulation in the design evaluation process: an exemplification of the use of a computer field model. In *Interflam 90*, pp. 55–66. London: Interscience.

di Blasi, C., Crescitelli, S., Russo, G. & Fernandez-Pello, A. C. 1988 Model of the flow assisted spread of flames over a thin charring combustible. In *22nd Symp. (Int.) Combustion*, pp. 1205–1212. Pittsburgh, PA: The Combustion Institute.

Favre, A. 1965 Equations des gaz turbulents compressibles. *J. Mechanique* **4**, 361–392.

Faeth, G. M., Jeng, S. M. & Gore, J. 1985 Radiation from fires. In *Heat transfer in fire and combustion systems* (ed. C. K. Law *et al.*), pp. 137–181. New York: American Society of Mechancial Engineers.

Gosman, A. D., Pun, W. M., Runchal, A., Spalding, D. B. & Wolfstein, M. 1969 *Heat and mass transfer in recirculating flows*. London: Academic.

Jones, W. P. & Whitelaw, J. H. 1982 Calculation methods for reacting turbulent flows: a review. *Combust. Flame.* **48**, 1–26.

Khan, I. M. & Greeves, G. 1974 A method for calculating the formation and combustion of soot in diesel engines. In *Heat transfer in flames* (ed. N. H. Afgan & J. M. Beer), pp. 289–404. New York: Wiley.

Lee, K. B., Thring, M. W. & Beer, J. M. 1962 On the rate of combustion of soot in a laminar flame. *Combust. Flame* **6**, 137–145.

Malalasekera, W. M. G. 1988 Mathematical modelling of fires and related processes. PhD thesis, Imperial College, London, UK.

Markatos, N. C., Malin, M. R. & Cox, G. 1982 Mathematical modelling of buoyancy induced smoke flow in enclosures. *Int. J. Heat Mass Transfer* **25**, 63–75.

Markstein, G. H. 1984 Relationship between smoke point and radiant emission from buoyant turbulent and laminar diffusion flames. In *20th Symp. (Int.) Combustion*, pp. 1055–1061. Pittsburgh, PA: The Combustion Institute.

Magnussen, B. F. & Hjertager, B. H. 1976 On mathematical modelling of turbulent combustion with special emphasis on soot formation and combustion. In *16th Symp. (Int.) Combustion*, pp. 719–729. Pittsburgh, PA: The Combustion Institute.

Modak, A. T. & Croce, P. A. 1977 Plastic pool fires. *Combust. Flame* **30**, 251–265.

Moss, J. B. 1995 Turbulent diffusion flames. In *Combustion fundamentals of fire* (ed. G. Cox), pp. 221–272. London: Academic.

Rodi, W. 1978 Turbulence models and their application in hydraulics-a state of the art review. SFB Report 80/T/125, University of Karlsruhe.

Sivathanu, Y. R. & Faeth, G. M. 1990*a* Generalised state relationships for scalar properties in nonpremixed hydrocarbon–air flames. *Combust. Flame* **82**, 211–230.

Sivathanu, Y. R. & Faeth, G. M. 1990*b* Soot volume fractions in the overfire region of turbulent diffusion flames. *Combust. Flame* **81**, 133–149.

Smith, N. S., Bilger, R. W. & Chen, J.-Y. 1992 Modelling of nonpremixed hydrogen jet flames using a conditional moment closure method. In *24th Symp. (Int.) Combustion*, pp. 263–269. Pittsburgh, PA: The Combustion Institute.

Spalding, D. B. 1971 Mixing and chemical reaction in steady state confined turbulent flames. In *13th Symp. (Int.) Combustion*, pp. 649–657. Pittsburgh, PA: The Combustion Institute.

Syed, K. J. 1990 Soot and radiation modelling in buoyant fires. PhD thesis, Cranfield University.

Tewarson, A., Lee, J. L. & Pion, R. F. 1981 The influence of oxygen concentration on fuel parameters for fire modelling. In *18th Symp. (Int.) Combustion*, pp. 563–570. Pittsburgh, PA: The Combustion Institute.

Viskanta, R. & Menguc, M. P. 1987 Radiation heat transfer in combustion systems. *Prog. Energy Combust. Sci.* **13**, 97–160.

PHILOSOPHICAL TRANSACTIONS OF THE ROYAL SOCIETY A MATHEMATICAL, PHYSICAL & ENGINEERING SCIENCES